

Nuclear spin-lattice relaxation of ^{62}Cu at low temperatures in iron

V. V. Golovko,^{1,*} I. S. Kraev,¹ T. Phalet,¹ N. Severijns,^{1,†} D. Vénos,² D. Zákoucký,² P. Herzog,³ C. Tramm,³ U. Köster,⁴ D. Srnka,² M. Honusek,² B. Delauré,¹ M. Beck,¹ V. Yu. Kozlov,¹ and A. Lindroth¹

¹*K.U.Leuven, Instituut voor Kern-en Stralingsfysica, B-3001 Leuven, Belgium*

²*Nuclear Physics Institute, ASCR, 250 68 Řež, Czech Republic*

³*Helmholtz-Institut für Strahlen-und Kernphysik, Universität Bonn, D-53115 Bonn, Germany*

⁴*ISOLDE, CERN, CH-1211 Genève 23, Switzerland*

(Received 8 March 2006; published 30 October 2006)

The nuclear spin-lattice relaxation of ^{62}Cu in iron has been studied with the low temperature nuclear orientation method. At temperatures ranging from 6.5 mK to about 100 mK and a magnetic field of 0.1 T the relaxation constant for ^{62}Cu in Fe was found to be $C_K[^{62}\text{Cu}] = 4.34(25)$ sK.

DOI: [10.1103/PhysRevC.74.044313](https://doi.org/10.1103/PhysRevC.74.044313)

PACS number(s): 23.20.En, 72.15.Lh, 71.20.Be, 75.50.Bb

I. INTRODUCTION

Nuclear spin-lattice relaxation (NSLR) rates of impurity elements in metals permit critical tests of electronic structure theory as they depend sensitively on the local density of states near the Fermi surface. In Ref. [1] the systematics of the NSLR of transition-element impurities in iron was discussed and experimental results were compared to *ab initio* calculations reported by Akai [2]. The experimental results had been obtained by a variety of experimental techniques using both stable and unstable nuclei. This revealed information about changes in the local density of states and the interactions of impurity d-electrons with the iron electronic bands. For most elements of the 3d-series (viz. Sc to Zn) the data turned out to be reliable and consistent. However, for the case of CuFe only a spin-echo nuclear magnetic resonance result obtained at a temperature of 4.2 K is available [3], mainly because of the short lifetimes for most of the Cu radionuclides, and the authors of Ref. [1] point out that an independent measurement would be desirable.

Good knowledge of the NSLR rate for copper in iron is also of interest to nuclear physics. Since pure Cu beams have recently become available from the RILIS laser ion source at ISOLDE [4,5], the Cu isotopes have raised interest for, e.g., nuclear moment measurements [6–9], isospin impurity studies [10], and beta-asymmetry measurements for weak interaction studies [11]. When applying the on-line low temperature nuclear orientation (LTNO) technique (as in Refs. [7–11]) which is a very effective spectroscopic method, good knowledge of the relaxation rate in iron is often required, especially when dealing with the shorter-lived Cu isotopes (see, e.g., Ref. [10]).

In this work we present a measurement of the NSLR rate for ^{62}Cu in Fe with the method of on-line LTNO [12] with continuous implantation, using the NICOLE ^3He - ^4He dilution refrigerator setup [13,14] at ISOLDE/CERN [15]. A review of various experimental techniques available for determining

NSLR rates of dilute impurities in ferromagnetic host materials can be found in Ref. [1]. The method of on-line LTNO used here deals with doses of typically about 10^{10} to 10^{12} at./cm², corresponding to low local impurity concentrations.

II. EXPERIMENTAL METHOD

The NSLR rate of ^{62}Cu in iron was determined from the asymmetry of β -radiation emitted by ^{62}Cu nuclei that were continuously implanted into an Fe host foil and were oriented in the NICOLE dilution refrigerator.

Detailed information on the EC/β^+ decay of ^{62}Cu ($T_{1/2} = 9.73$ min, $I^\pi = 1^+$) can be found in Ref. [16]. The strongest β -decay branch of ^{62}Cu is an allowed $1^+ \rightarrow 0^+$ Gamow-Teller transition, with endpoint energy $E_0 = 2926$ keV and intensity of 97.2%, to the stable ground state of ^{62}Ni . The rest of the β -decay intensity is spread over at least nine other very weak branches that can be neglected here.

The radioactive ^{62}Cu was produced at ISOLDE (CERN) with a 1.4 GeV proton beam from the Proton Synchrotron Booster, bombarding a ZrO₂ felt target (6.3 g Zr/cm²) [17] connected to the RILIS laser ion source [4] which provided the required element selectivity for the separation of ^{62}Cu . After ionization and acceleration to 60 keV, the ^{62}Cu beam was mass-separated by the General Purpose Separator, transported through the beam distribution system, and implanted into a polished and annealed 99.99% pure Fe foil (thickness 250 μm) that was soldered onto the cold finger of the NICOLE ^3He - ^4He dilution refrigerator. The total dose was about 3×10^{12} atoms/cm² corresponding to a Cu concentration of about 20 ppm. The iron foil was magnetized by an external magnetic field generated by a superconducting split-coil magnet. Firstly, a field $B_{\text{ext}} = 0.5$ T was applied in order to magnetically saturate the iron foil. This was thereafter reduced to 0.10(2) T so as to minimize its influence on the trajectories of the β -particles.

The angular distribution of the positrons emitted during the β^+ -decay of ^{62}Cu was observed with three high purity Ge (HPGe) particle detectors with a sensitive diameter of 12 mm and a thickness of 5 mm that were produced and tested in the Nuclear Physics Institute in Řež [18,19]. They were installed at a distance of about 32 mm from the sample, inside

*Present address: Cyclotron Institute, Texas A&M University, College Station, Texas 77843, USA.

†Electronic address: nathal.severijns@fys.kuleuven.be

the 4 K radiation shield of the refrigerator. The fact that they were looking directly at the radioactive source assured good counting rates and at the same time avoided the effects of scattering or absorption of the β -particles in radiation shields. The detectors operated at a temperature of about 10 K. In order to minimize the effects of scattering in the Fe foil they were mounted to view the foil surface, which was parallel to the magnetic field, under an angle of about 15° . They were connected with thin isolated copper wires (about 12–14 cm long) to the preamplifiers outside the refrigerator. Thin wires were used in order to minimize the heat load from room temperature to the detectors. The energy resolution was about 3 keV for 1 MeV β -particles.

Apart from these particle detectors, large-volume HPGe detectors for detection of the γ -radiation were installed outside the refrigerator at 0° , 90° , and 180° with respect to the orientation axis (magnetic field axis). The typical energy resolution of these was about 3 keV for the 1332 keV γ -line of ^{60}Co . All data were corrected for the “dead time” of the data acquisition system using a precision pulse generator.

The spatial distribution of radiation emitted by oriented nuclei can be described by the angular distribution function [20]

$$W(\theta) = 1 + f \sum_{\lambda} B_{\lambda} U_{\lambda} A_{\lambda} Q_{\lambda} P_{\lambda}(\cos \theta). \quad (1)$$

Here f represents the fraction of nuclei that experience the full hyperfine interaction, while the rest ($1 - f$) is supposed to experience no interaction at all. B_{λ} are the nuclear orientation parameters which depend on the magnetic moment μ of the decaying nuclei, the total magnetic field B these nuclei experience (i.e., the sum of the hyperfine magnetic field B_{hf} , the applied field B_{app} , and the demagnetization field B_{dem}), the temperature of the sample T , and the initial spin I , the lifetime and the relaxation constant C_K of the oriented state. The U_{λ} are the deorientation coefficients, which account for the effect of unobserved intermediate radiations, while A_{λ} are the directional distribution coefficients which depend on the properties of the observed radiation itself. Finally, Q_{λ} are solid angle correction factors and $P_{\lambda}(\cos \theta)$ are the Legendre polynomials. The angle θ is measured with respect to the orientation axis.

For γ -rays only λ even terms occur. For positrons from allowed β -decays only the $\lambda = 1$ term is present and Eq. (1) transforms to

$$W(\theta) = 1 + f \frac{v}{c} B_1 A_1 Q_1 \cos \theta, \quad (2)$$

where v/c is the positron velocity relative to the speed of light (note that the dependence of the anisotropy on v/c was explicitly included in $W(\theta)$ here, whereas in Ref. [20] it is included in A_1). In our experiment ^{62}Cu nuclei were implanted continuously. Therefore, B_1 results from an equilibrium between implantation of warm, unoriented, nuclei and the decay of (partially) relaxed nuclei (see Sec. III) since the half-life and relaxation time are of the same order of magnitude.

In order to take into account the rather short half-life of ^{62}Cu as well as possible beam fluctuations the ratio $W(15^\circ)/W(165^\circ)$ was determined experimentally. The

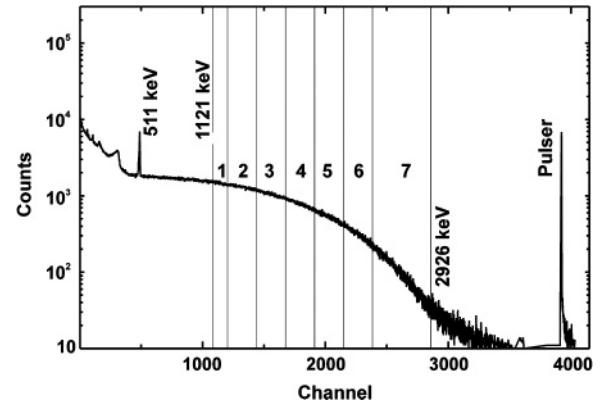


FIG. 1. β -spectrum for unoriented (“warm”) ^{62}Cu obtained in 300 s with one of the HPGe particle detectors. The 511 keV γ -line, the β -spectrum endpoint at 2926 keV and the pulser peak are indicated. The part of the β -spectrum that was used for analysis is the region between 1121 keV and the endpoint. It was subdivided in seven energy bins.

anisotropy function R is then given by

$$R = \frac{W(15^\circ)}{W(165^\circ)} = \frac{\left[\frac{N(15^\circ)}{N(165^\circ)} \right]_{\text{cold}}}{\left[\frac{N(15^\circ)}{N(165^\circ)} \right]_{\text{warm}}}, \quad (3)$$

where $N(\theta)_{\text{cold}}$ and $N(\theta)_{\text{warm}}$ are the “cold” (i.e., polarized; millikelvin temperatures), and “warm” (i.e., unpolarized; $T > 1$ K) β -particle count rates.

The temperature of the sample was determined from the anisotropy of the 136 keV γ -ray of a calibrated $^{57}\text{Co}/\text{Fe}$ nuclear orientation thermometer [21].

Figure 1 shows a “warm” (i.e., no orientation) β -spectrum of ^{62}Cu obtained with one of the HPGe particle detectors. In determining the β -anisotropies for the different energy regions special care had to be taken to subtract the background under the β -spectrum. The absolute efficiency for the detection of γ -rays in the energy region of interest did not exceed a few percent [22]. Since there were no radioactive contaminants in the beam and no intense γ -rays are present in the decay of ^{62}Cu itself, most of the background in the part of the β -spectrum that was used for analysis was due to backscattering of positrons on the detectors and summing with Compton scattered 511 keV γ -rays from annihilation of positrons in the sensitive volume of the particle detectors. This background was evaluated using the method described in Ref. [22] (see also Ref. [23]).

III. RESULTS AND DISCUSSION

The observed β -asymmetry was fitted simultaneously for the fraction f and the spin-lattice relaxation constant C_K via the orientation parameter B_1 [24]. The parameter f is independent of temperature and determines only the size of the anisotropy effect $|R - 1|$, while B_1 is temperature dependent and therefore determines the shape of the anisotropy R versus temperature. The calculation of B_1 takes into account that directly after implantation the nuclei have polarization zero. In the time following they relax to thermal equilibrium with

the cold lattice and one has a competition between nuclear decay and relaxation which determines the size of B_1 .

C_K describes the relaxation for the case of a dominant magnetic-dipole relaxation mechanism, as applies to the 3d impurities in an Fe host [1]. In conventional nuclear magnetic resonance (NMR) at lattice temperatures $T \geq 1$ K, spin-lattice relaxation leads to an exponential time dependence of the signal and a relaxation time T_1 can be defined unambiguously. Such experiments are always performed in the high temperature limit, i.e., $T \gg T_{\text{int}}$ with the interaction temperature T_{int} given by the nuclear level splitting:

$$T_{\text{int}} = |\mu B_{\text{tot}}/k_B I| \quad (4)$$

(with k_B the Boltzmann constant), such that for metallic samples the Korringa law, i.e., $C_K = T_1 T$, is valid. The relaxation behavior we probe via the B_1 orientation parameter is the same as in conventional NMR. Further, since $T_{\text{int}}(^{62}\text{CuFe}) = 3.0$ mK (see below) and our data were taken at temperatures between about 100 mK and 6.5 mK, the high temperature limit applies.

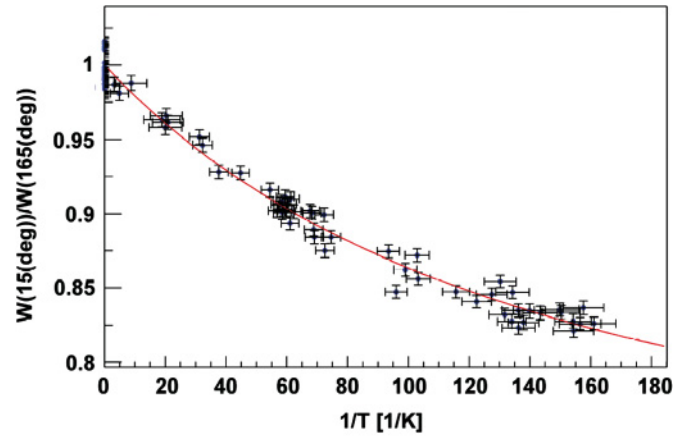
In order to take into account the effect of spin-lattice relaxation (i.e., C_K) in Eq. (1) the nuclear orientation parameter B_1 was expressed as $\rho_1 B_1(\text{th})$, with $\rho_1 = B_1(\text{sec})/B_1(\text{th})$ the ratio of the observed orientation parameter $B_1(\text{sec})$ for the nuclear ensemble when in secular equilibrium and the thermal equilibrium orientation parameter $B_1(\text{th})$. The ρ_1 attenuation coefficients were determined according to the procedure outlined in Ref. [24] (see also Ref. [25]) and taking into account the observed temperature for each individual data point.

In fitting the experimental data we used $\mu(^{62}\text{Cu}) = -0.380(4) \mu_N$ [26] and $B_{\text{hf}}(\text{CuFe}) = -21.8(1)$ T (see Ref. [7] and references therein). The demagnetization field was calculated to be $B_{\text{dem}} = 0.037(5)$ T for the Fe foil used here (see Ref. [10]). For the $1^+ \rightarrow 0^+ \beta^+$ decay of ^{62}Cu , $A_1 = \sqrt{I + 1/3I} = -0.8165$, with I the spin of the ground state of ^{62}Cu . The Q_1 factors (Table I) were calculated using the {GEANT4} [27] Monte Carlo simulation code, for the seven energy bins considered in the analysis and for both particle detectors. Details of these calculations are outlined in Ref. [10]. The uncertainties on the Q_1 -factors take into account the precision to which the detector geometry was determined, scattering effects, the influence of the external magnetic field on the β -particle trajectories, as well as the Monte Carlo statistical error, with the last one giving the largest contribution.

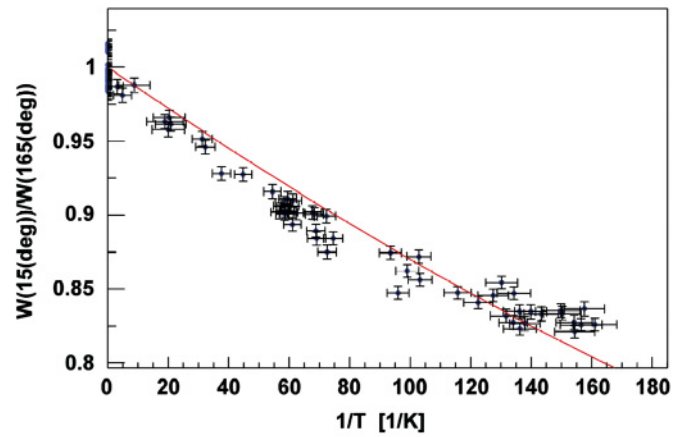
The results obtained for C_K and f from fitting the theoretical function to $W(15^\circ)/W(165^\circ)$ for all energy bins are

TABLE I. Q_1 factors (calculated with GEANT4) for the 15° and 165° particle detectors in the seven energy bins, ranging from 1121 keV to the β -spectrum endpoint of ^{62}Cu , and results for the relaxation constant C_K and the f -factor when fitting the $W(15^\circ)/W(165^\circ)$ -anisotropies for these energy bins (see Fig. 1).

Bin	1	2	3	4	5	6	7
Energy (keV)	1121–1241	1241–1482	1482–1723	1723–1964	1964–2205	2205–2446	2446–2926
$Q_1^{15^\circ}$	0.842(11)	0.854(4)	0.899(7)	0.928(10)	0.935(7)	0.960(13)	0.976(5)
$Q_1^{165^\circ}$	0.887(15)	0.866(14)	0.918(3)	0.940(6)	0.963(6)	0.967(9)	0.982(9)
f	0.66(4)	0.69(3)	0.63(3)	0.65(3)	0.61(3)	0.55(4)	0.52(8)
C_K [s K]	4.2(6)	4.5(6)	4.1(5)	4.8(5)	4.0(6)	3.2(8)	2.8(15)



(a) with C_K



(b) without C_K

FIG. 2. (Color online) (a) $W(15^\circ)/W(165^\circ)$ values versus inverse temperature for positrons from $^{62}\text{CuFe}$ with energies between 1482 and 1723 keV (bin 3 in Fig. 1) [10]. The curve is a fit to the data varying both f and C_K yielding $f = 0.63(3)$ and $C_K = 4.1(5) \text{ s K}$ ($\chi^2/\nu = 3.0$). (b) Same data as in (a) together with the fitted curve that was obtained when $C_K = 0$ was assumed (i.e. using thermal equilibrium values for B_1) and with f being the only free parameter. This fit yielded $f = 0.412(7)$ ($\chi^2/\nu = 9.3$). Note that since the χ^2/ν values are larger than unity the errors obtained from the fits have been increased by the factor $\sqrt{\chi^2/\nu}$.

listed in Table I. The fit for the energy region 1482–1723 keV is shown in Fig. 2 as an example. As can be seen the fitted values for the last two energy bins are significantly lower than those

TABLE II. Experimental values for the relaxation constant C_K and the reduced relaxation rate r for the systems $^{62}\text{CuFe}$ and $^{63}\text{CuFe}$ at $B_{\text{app}} = 0.1$ T [Eq. (7)] and in the high-field limit (i.e., $C_{K\infty}$ and r_∞), compared with predictions from the empirical rule [Eq. (7)] [30] and with a theoretical value [2].

	$C_{K,0.1T}^{\text{exp}}$ sK	$C_{K\infty}^{\text{exp}}$ sK	$C_{K\infty}^{\text{emp}}$ sK	$r_{0.1T}^{\text{exp}}$ $\times 10^{15} \text{ T}^2\text{s/K}$	r_∞ $\times 10^{15} \text{ T}^2\text{s/K}$
$^{62}\text{CuFe}$	4.34(25) ^a	10.9(14) ^b	15.6 ^c	0.70(4) ^d	0.28(4) ^e
$^{63}\text{CuFe}$	0.422(23) ^f	1.11(12) ^g	1.0 ^c	0.469(26) ^d	0.178(20) ^e
CuFe					0.22 ^h

^aThis work.

^bFrom column 2 and Eq. (6).

^cCalculated with Eq. (7).

^dFrom column 2 and Eq. (8).

^eFrom column 3 and Eq. (8).

^fFrom Fig. 5 in Ref. [3].

^gFrom Table I in Ref. [3].

^hTheoretical prediction using the KKR-Green's function method [2].

for the first five bins, although they are still in agreement within the large error bars. This is an indication for the background subtraction not being perfect. This is not a problem for the first five energy bins where the background constitutes only a small part of the total intensity, but becomes important in the highest energy part of the β -spectrum where the count rate decreases rather fast. Considering then only the first five energy bins, the weighted average value for the relaxation constant in the temperature range from 6.5 mK to about 100 mK is found to be

$$C_{K,0.1T}[^{62}\text{Cu}] = 4.34 \pm 0.25 \text{ s K} \quad (5)$$

[when considering all seven energy bins $C_K = 4.21(23)$ s K is obtained].

In Table II our result for the relaxation constant C_K for $^{62}\text{CuFe}$ in the millikelvin region and the result reported in Ref. [3] for $^{63}\text{CuFe}$ ($\mu = 2.227\mu_N$, $I = 3/2$) from a spin-echo measurement at 4.2 K are compared to each other (columns 2 and 3) as well as to the empirical high-field limiting values for the relaxation constant, viz. $C_{K\infty}^{\text{emp}}$ (in column 4), and to a theoretical value for the relaxation rate of Cu in Fe (column 6).

Here we are assuming that the implanted copper nuclei which contribute to our signal occupy the same, i.e., the substitutional, lattice site as those which were thermally introduced into iron in Ref. [3]. For implanted nuclei this is inferred from successful NMR on oriented nuclei with the same sample preparation technique as in this work [9]. For the thermally prepared samples of Ref. [3] this is inferred from the preparation technique used, combined with the solubility limits for copper in iron (solubility more than about 1% at. at 800 °C) [28]. The NSLR of stable and unstable nuclei in a given lattice is of course the same.

To obtain the high-field limit values ($C_{K\infty}^{\text{exp}}$) listed in column 3 we used the well known fact that the relaxation rate is magnetic field dependent and saturates at fields of 0.5 T to 1 T (high-field limit) [1,3,29]. If one takes fig. 5 of Ref. [3] to be the correct field dependence, the relaxation rate ($\propto C_K^{-1}$)

for Cu in Fe at the field of 0.1 T used here is found to be faster than in high fields by a factor of

$$\frac{C_{K\infty}}{C_{K,0.1T}} = 2.5(3). \quad (6)$$

The empirical relaxation constants ($C_{K\infty}^{\text{emp}}$) in column 4 were calculated from the relation

$$C_{K\infty}^{\text{emp}} T_{\text{int}}^2 = 1.4 \cdot 10^{-4} \text{ s K}^3 \quad (7)$$

that was deduced for transition element impurities in an Fe host lattice [30]. This relation was found to reproduce the majority of the experimental data within a factor of about 2.5, the maximum deviation being a factor of 4 [30,31].

As can be seen (column 2) the spin-lattice relaxation is found to proceed a factor of about 10 slower for $^{62}\text{CuFe}$ compared to $^{63}\text{CuFe}$ due to the smaller hyperfine interaction strength for $^{62}\text{CuFe}$ (i.e., $T_{\text{int}} = 3.0$ mK for $^{62}\text{CuFe}$ and 11.8 mK for $^{63}\text{CuFe}$). The high-field limiting values for the relaxation constant, i.e., $C_{K\infty}^{\text{exp}}$, for both isotopes (column 3) agree well with those obtained from the empirical relation [Eq. (7) and column 4].

An isotope (viz. g -factor) independent measure of the NSLR rate is the reduced relaxation rate constant

$$r = \frac{0.436 \times 10^{-15}}{C_K g^2} \text{ T}^2\text{s/K} \quad (8)$$

with C_K in units of s K and g being the g -factor [30]. The reduced relaxation rates r for both isotopes are listed in columns 5 (for $B_{\text{app}} = 0.1$ T) and 6 (high field limit). They differ by a factor of about 1.5. In column 6 also the theoretical prediction for r_∞ for CuFe of Akai [2], using the KKR Green's function method, is listed. While the value of r_∞ obtained for $^{63}\text{CuFe}$ in Ref. [3] is smaller than this theoretical prediction, our result is slightly larger. This effect could be due to the very different Cu concentration (i.e., dilute versus alloy) in both experiments, where the result of this work should then be taken as the low concentration limit.

In conclusion we have determined the relaxation rate of Cu in host iron for a highly dilute system (i.e., with a concentration of about 20 ppm) and at millikelvin temperatures using nuclear orientation with continuous implantation and β -particle detection. The value of the relaxation constant is about 50% higher than that of a pulsed NMR experiment with a 1% Cu-Fe alloy at 4.2 K [3]. It is also slightly larger than the theoretical prediction of Akai [2], in accord with the results for some lighter 3d impurities in iron (table 1 of ref. [1]). It would

be interesting to see whether improved theoretical calculations can reproduce this behavior.

ACKNOWLEDGMENTS

This work was supported by the Fund for Scientific Research Flanders (FWO), the IHRP program of the European Commission (contract no. HPRI-CT-1999-00018) and the Grant Agency of the Czech Republic.

-
- [1] T. Funk, E. Beck, W. Brewer, C. Bobek, and E. Klein, *J. Magn. Magn. Mater.* **195**, 406 (1999).
- [2] H. Akai, *Hyperfine Interact.* **43**, 255 (1988).
- [3] M. Kontani, T. Hioki, and Y. Masuda, *J. Phys. Soc. Jpn.* **32**, 416 (1972).
- [4] U. Köster, V. N. Fedoseyev, and V. I. Mishin, *Spectrochim. Acta B* **58**, 1047 (2003).
- [5] U. Köster, V. Fedoseyev, V. Mishin, L. Weissman, M. Huyse, K. Kruglov, W. Mueller, P. Van Duppen, J. Van Roosbroeck, P. Thirolf, H. Thomas, D. Weisshaar, W. Shulze, R. Borcea, M. La Commara, H. Schatz, K. Schmidt, S. Röttger, G. Huber, V. Sebastian, K. Kratz, R. Catherall, U. Georg, J. Lettry, M. Oinonen, H. Ravn, H. Simon, and ISOLDE Collaboration, *Nucl. Instrum. Methods B* **160**, 528 (2000).
- [6] L. Weissman, U. Köster, R. Catherall, S. Franchoo, U. Georg, O. Jonsson, V. N. Fedoseyev, V. I. Mishin, M. D. Seliverstov, M. Huyse, K. Kruglov, P. VanDuppen, and J. VanRoosbroeck, *Phys. Rev. C* **65**, 024315 (2002).
- [7] J. Rikovska, T. Giles, N. J. Stone, K. van Esbroeck, G. White, A. Wöhr, M. Veskovíc, I. S. Towner, P. F. Mantica, J. I. Prisciandaro, D. J. Morrissey, V. N. Fedoseyev, V. I. Mishin, U. Köster, and W. B. Walters, *Phys. Rev. Lett.* **85**, 1392 (2000).
- [8] J. Rikovska and N. J. Stone, *Hyperfine Interact.* **129**, 131 (2000).
- [9] V. V. Golovko, I. Kraev, T. Phalet, N. Severijns, B. Delauré, M. Beck, V. Kozlov, A. Lindroth, S. Versyck, D. Zákoucký, D. Vénos, D. Srnka, M. Honusek, P. Herzog, C. Tramm, U. Köster, and I. S. Towner, *Phys. Rev. C* **70**, 014312 (2004).
- [10] V. V. Golovko, Ph.D. thesis, Katholieke Universiteit Leuven (2005), <http://hdl.handle.net/1979/43>.
- [11] N. Severijns *et al.*, CERN document CERN-INTC-2004-027.
- [12] *Low-Temperature Nuclear Orientation*, edited by H. Postma and N. J. Stone (North-Holland, Amsterdam, 1986).
- [13] K. Schlösser, I. Berkes, E. Hagn, P. Herzog, T. Niinikoski, H. Postma, C. Richard-Serre, J. Rikovska, N. J. Stone, L. Vanneste, E. Zech, and the ISOLDE and NICOLE Collaborations, *Hyperfine Interact.* **43**, 141 (1988).
- [14] J. Wouters, N. Severijns, J. Vanhaverbeke, W. Vanderpoorten, and L. Vanneste, *Hyperfine Interact.* **59**, 59 (1990).
- [15] E. Kugler, *Hyperfine Interact.* **129**, 23 (2000).
- [16] H. Junde and B. Singh, *Nucl. Data Sheets* **91**, 317 (2000).
- [17] U. Köster, U. C. Bergmann, D. Carminati, R. Catherall, J. Cederkäll, J. G. Correia, B. Crepieux, M. Dietrich, K. Elder, V. Fedoseyev, L. Fraile, S. Franchoo, H. Fynbö, U. Georg, T. Giles, A. Joinet, O. C. Jonsson, R. Kirchner, C. Lau, J. Lettry, H. J. Maier, V. I. Mishin, M. Oinonen, L. Peräjärvi, H. L. Ravn, T. Rinaldi, M. Santana-Leitner, U. Wahl, L. Weissman, and the ISOLDE Collaboration, *Nucl. Instrum. Methods B* **204**, 303 (2003).
- [18] D. Vénos, A. Van Assche-Van Geert, N. Severijns, D. Srnka, and D. Zákoucký, *Nucl. Instrum. Methods A* **454**, 403 (2000).
- [19] D. Zákoucký, D. Srnka, D. Vénos, V. V. Golovko, I. Kraev, T. Phalet, P. Schuurmans, N. Severijns, B. Vereecke, S. Versyck, and the NICOLE/ISOLDE Collaboration, *Nucl. Instrum. Methods A* **520**, 80 (2004).
- [20] K. S. Krane in *Low-Temperature Nuclear Orientation*, edited by N. J. Stone and H. Postma (North-Holland, Amsterdam, 1986), Chap. 2.
- [21] H. Marshak, in *Low-Temperature Nuclear Orientation*, edited by N. J. Stone and H. Postma (North-Holland, Amsterdam, 1986), Chap. 16.
- [22] N. Severijns, D. Vénos, P. Schuurmans, T. Phalet, M. Honusek, D. Srnka, B. Vereecke, S. Versyck, D. Zákoucký, U. Köster, M. Beck, B. Delauré, V. Golovko, and I. Kraev, *Phys. Rev. C* **71**, 064310 (2005).
- [23] D. M. Rehfield and R. B. Moore, *Nucl. Instrum. Methods* **157**, 365 (1978).
- [24] D. Vénos, D. Zákoucký, and N. Severijns, *At. Data Nucl. Data Tables* **83**, 1 (2003).
- [25] T. L. Shaw and N. J. Stone, *Hyperfine Interact.* **43**, 299 (1988).
- [26] E. Phillips and A. Jackson, *Phys. Rev.* **169**, 917 (1968).
- [27] S. Agostinelliae, J. Allisonas, K. Amakoe, J. Apostolakisa, H. Araujoaj, P. Arcel, M. Asaig, D. Axeni, S. Banerjeebi, G. Barrandan, F. Behnerl, and L. Bellagambac, *Nucl. Instrum. Methods A* **506**, 250 (2003).
- [28] M. Hansen and K. Anderko, *Constitution of Binary Alloys*, (McGraw-Hill, New York, 1958).
- [29] M. Kopp and E. Klein, *Hyperfine Interact.* **11**, 153 (1981).
- [30] E. Klein, in *Low-Temperature Nuclear Orientation*, edited by N. J. Stone and H. Postma (North-Holland, Amsterdam, 1986), Chap. 12.
- [31] E. Klein, *Hyperfine Interact.* **15/16**, 557 (1983).